

## Supplemental Data

# Low-Dose T<sub>3</sub> Replacement Restores Depressed Cardiac T<sub>3</sub> Levels, Preserves Coronary Microvasculature and Attenuates Cardiac Dysfunction in Experimental Diabetes Mellitus

Nathan Y Weltman,<sup>1</sup> Kaie Ojamaa,<sup>2</sup> Evelyn H Schlenker,<sup>1</sup> Yue-Feng Chen,<sup>4</sup> Riccardo Zucchi,<sup>3</sup> Alessandro Saba,<sup>3</sup> Daria Colligiani,<sup>3</sup> Viswanathan Rajagopalan,<sup>4</sup> Christine J Pol,<sup>4</sup> and A Martin Gerdes<sup>4</sup>

Online address: <http://www.molmed.org>

The Feinstein Institute  
for Medical Research   
Empowering Imagination. Pioneering Discovery.\*

### SUPPLEMENTARY MATERIALS AND METHODS

#### Tissue Collection

Following terminal experiments, each animal was deeply anesthetized with 5% isoflurane and the chest cavity was opened. Hearts were quickly excised and vessels were relaxed, flushed of remaining blood, and hearts were arrested in diastole by aortic retrograde perfusion with solution containing 0.2% 2, 3- butanedione monoxime (BDM), 0.1% adenosine, and heparin dissolved in phosphate buffered saline (PBS). Samples were rinsed in ice cold PBS, trimmed, blotted and weighed. LV apical and basal transverse slices were flash frozen in liquid nitrogen and stored at -80° C. The remaining tissue was sliced transversely and either immersion fixed in ice cold 10% formalin or embedded in OCT compound (Sakura Finetek Inc.; Torrance, CA) and frozen.

#### Measurement of Blood Glucose Levels

Blood glucose (BG) levels were measured using an Ascensia Contour blood glucose meter (Bayer, Pittsburgh, PA). Eight days after STZ/N, fasting blood samples from the tail vein were used to confirm elevated blood glucose levels and DM (Supplementary Figure 1). Due to animal welfare concerns from University of South Dakota Animal Care and Use Committee and the school veterinar-

ian, we were not allowed to fast the animals prior to sacrifice. Therefore, non-fasted blood samples were obtained from the LV after terminal procedures and thoracotomy. As expected, the non-fasted state and increased stress/trauma associated with terminal experiments and thoracotomy led to significant blood glucose elevations in all groups. Although values were elevated in all groups, control values were significantly lower than the two DM groups (Supplementary Table 2).

#### Measurement of Cardiac Tissue TH Levels

THs were extracted from LV tissue homogenates and analysed by HPLC tandem mass spectrometry using previously described methods with minor modifications (1, 2). Briefly, Pooled LV (~350-500 mg) homogenates were spiked with 5 pmol of each of the following internal standards: <sup>13</sup>C<sub>6</sub>-T<sub>3</sub>, <sup>13</sup>C<sub>6</sub>-T<sub>4</sub> (IsoSciences, King of Prussia, PA). THs were extracted using Bond Elut Certify SPE (Agilent Technologies, Santa Clara, CA) and converted into their butyl esters. THs were then separated and quantified using HPLC tandem mass spectrometry isotope dilution method.

#### Echocardiographic Measurements

Echocardiography was performed in each animal prior to sacrifice using a Vevo 770 high-resolution imaging system with RMV710B transducer (Visualsonics;

Toronto, Canada) as previously described (3). Briefly, rats were anesthetized using isoflurane (1.5%) and two-dimensional echocardiograms were obtained from short-axis views of the left ventricle (LV) at the level of the papillary muscle tips. Two dimensional M-mode echocardiograms were used to measure the LV dimensions in systole and diastole. Fractional shortening (FS) was calculated as FS = [(LVIDd-LVIDs)/LVIDd] × 100.

#### LV Hemodynamic Measurements

LV hemodynamics were obtained by catheterization of the right carotid artery using a Millar Micro-tip catheter (Millar Instruments; Houston, TX) as described previously (4, 5). After stabilization, LV and aortic measurements were recorded and processed electronically by a MPVS-400 pressure volume unit (Millar Instruments; Houston, TX) and recorded electronically using Chart 7 software (ADInstruments Inc., Colorado Springs, CO).

#### REAL-TIME PCR

RNA was isolated using TRIzol reagent followed by RNA purification using Pure-Link RNA mini kit and DNaseI kit (Invitrogen, Carlsbad, CA) as previously described (6). RNA quantity and quality were determined using a NanoDrop 1000 (Thermo Scientific, Wilmington, DE) and Agilent 2100 Bioanalyzer (Agilent Technologies, Santa Clara, CA). Equal amounts of RNA

from each sample were converted to cDNA using RT<sup>2</sup> First Strand Kit (SABiosciences, Frederick, MD). Gene expression was evaluated by a custom designed primer plate (Cat #: CAPR10931G; SABiosciences) or commercially available primers (SABiosciences) for deiodinase induction pathways, fetal genes, TH transporters, vascular growth regulators, and LV collagens using SYBR green/ROX detection. Gene expression was normalized using the housekeeping genes *Cyclophilin A* and *Rplp1*. Expression data was analysed using SABiosciences expression analysis online software.

### WESTERN BLOTTING

LV lysates were prepared with Laemmli buffer containing 5% β-mercaptoethanol and evenly loading onto SDS-PAGE gels. Protein was transferred to PVDF membranes and detected by the following antibodies (Developmental Studies Hybridoma Bank, University of Iowa: mAB F59 for total myosin heavy chain (MHC) and mAB s58 for MHC beta; Pierce antibodies (Thermo Fisher Scientific, Rockford, IL): SERCA2a (2A7-A1), PLB (MA3-919); Bradilla (Leeds, UK): p-PLB serine-16 (A010-12), p-PLB Threonine-17 (A010-13) followed by appropriate IgG-HRP secondary antibodies. Resultant bands were detected using chemiluminescence and captured using Kodak Image Station 4000MM Pro (Carestream Health, Inc., New Haven, CT). Band densitometry was quantified using Quantity One software (Bio-Rad, Hercules, CA) and normalization to the density of non-specific background band detected by reversible Ponceau S staining of the same blots.

### HISTOLOGY

Formalin fixed paraffin embedded mid-wall LV tissue sections (5-7 μm) were used to evaluate changes in LV microvasculature, fibrosis, and DIO3 deiodinase expression. Sections were deparaffinized by incubation with xylene and rehydrated with graded ethanol (100, 95, 85, 70%). LV tissue sections were then placed in IHC select citrate buffer, pH 6.0 (EMD Millipore, Billerica, MA) and boiled in a rice cooker for 20 min for antigen re-

trieval. All images were captured using an Olympus BX53 and cellSens imaging software (Olympus, Tokyo, Japan).

**Quantification of Capillaries and Small Arteriolar Resistance Vessels** - LV tissue sections were stained as previously described (6). FITC conjugated Isolectin B4 (IB4; Vector Labs, Burlingame, CA) and Cy3 conjugated α-smooth muscle actin (α-SMA; Sigma, St. Louis, MO) were used in combination to label endothelial cells and vascular smooth muscle cells respectively. Arteriolar numeric density (ND) was calculated from 30-35 random fields per heart as the average number of arterioles per total tissue area. Arteriolar length density (LD) was calculated based on the following formula:  $LD (mm/mm^3) = \sum(A/B)/M$ , where A and B are the maximum and minimum external arteriolar diameters, and M is the total tissue area (7). Arterioles with B dimensions between 5-30 μm were used to calculate arteriolar ND and LD. Capillary numeric density was determined from LV myocyte areas containing only circular, cross-sectioned capillary profiles stained with IB4-FITC and α-SMA-Cy3. The number of IB4 positive (and α-SMA negative) capillaries was normalized to total tissue area. Total capillary length was calculated as capillary ND x LV weight (6).

**LV DIO3 Deiodinase Staining and Quantification** - LV tissue sections were stained for DIO3 using a commercially available IHC detection kit (Epitomics, Burlingame, CA). Following antigen retrieval, endogenous peroxidase activity was blocked using peroxidase quenching solution. Sections were blocked with blocking solution for 1 h at RT, followed by a previously validated rabbit anti-DIO3 antibody (8-10) (Novus Biologicals, Littleton, CO) overnight at 4<sup>o</sup> C. Sections were then incubated for 30 min with HRP secondary antibody conjugate. 3, 3'-diaminobenzidine (DAB) was used as chromagen. Specificity was confirmed using an equivalent concentration of rabbit IgG instead of primary antibody. All images were quantified at 2x magnification using Image Pro software (MediaCybernetics, Rockville, MD). DIO3 was then expressed as % of staining versus the total tissue area.

**Myocardial Fibrosis Staining and Quantification** - LV tissue sections were stained with Masson's trichrome for visualization of myocardial fibrosis. Following deparaffinization and rehydration, slides were placed in Bouin's solution overnight at RT. Slides were then incubated with Weigert's working iron haematoxylin, followed by Biebrich Scarlet Acid Fuchsin. After incubation in Phosphomolybdic/phosphotungstic acid solution, slides were directly transferred to Aniline Blue solution. Slides were then incubated in 1% acetic acid, dehydrated and covered with Permount and coverslipped. Values represented as the proportion of collagen normalized to the total tissue area calculated using Image Pro Plus (Media Cybernetics, Bethesda, MD).

### SUPPLEMENTARY REFERENCES

1. Saba A, Chiellini G, Frascarelli S, et al. (2010) Tissue distribution and cardiac metabolism of 3-Iodothyronamine. *Endocrinology* 151: 5063-5073.
2. Pol C, Muller A, Zuidwijk M, et al. (2011) Left-Ventricular Remodeling After Myocardial Infarction Is Associated with a Cardiomyocyte-Specific Hypothyroid Condition. *Endocrinology* 152: 669-679.
3. Tamura T, Said S, Harris J, Lu W, Gerdes A. (2000) Reverse remodeling of cardiac myocyte hypertrophy in hypertension and failure by targeting of the renin-angiotensin system. *Circulation* 102: 253-259.
4. Zimmer H, Gerdes A, Lortet S, Mall G. (1990) Changes in heart function and cardiac cell size in rats with chronic myocardial infarction. *J. Mol. Cell. Cardiol.* 22: 1231-1243.
5. Weltman N, Wang D, Redetzke R, Gerdes A. (2012) Longstanding Hyperthyroidism is associated with normal or enhanced intrinsic cardiomyocyte function despite decline in global cardiac function. *Plos One* 7: e46655.
6. Savinova O, Liu YH, Aasen G, et al. (2011) Thyroid hormone promotes remodeling of coronary resistance vessels. *Plos One* 6: e25054.
7. Adair T, Wells M, Hang J, Montani J. (1994) A stereological method for estimating length density of the arterial vascular system. *Am. J. Physiol.* 266: H1434-H1438.
8. Freitas B, Gereben B, Castillo M, et al. (2010) Paracrine signaling by glial cell-derived triiodothyronine activates neuronal gene expression in the rodent brain and human cells. *J. Clin. Invest.* 120: 2206-2217.
9. Medina M, Molina J, Gadea Y, et al. (2011) The Thyroid Hormone-Inactivating Type III Deiodinase Is Expressed in Mouse and Human beta-Cells and Its Targeted Inactivation Impairs Insulin Secretion. *Endocrinology* 152: 3717-3727.
10. Shukla PK, Sittig LJ, Ullmann TM, Redei EE. (2011) Candidate Placental Biomarkers for Intrauterine Alcohol Exposure. *Alcoholism-Clinical and Experimental Research* 35: 559-565.

Supplementary Table S1. Primers used for gene expression experiments.

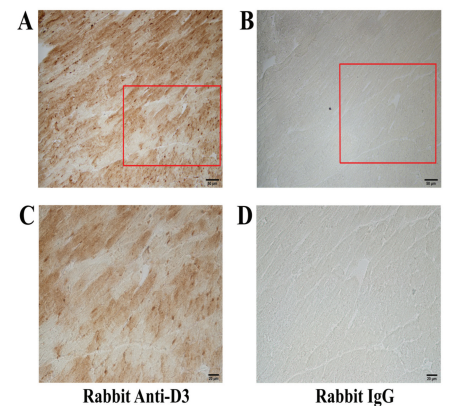
	Gene	Refseq #	Reference Position
Thyroid receptor $\beta$	<i>TR<math>\beta</math></i>	NM_012672	1174
Thyroid receptor $\alpha$	<i>TR<math>\alpha</math></i>	NM_031134	1331
Sarco(endo)plasmic reticulum ATPase II	<i>SERCA2a</i>	NM_001110139	3130
Myosin heavy chain $\alpha$	<i>Myh6</i>	NM_017239	3012
Myosin heavy chain $\beta$	<i>Myh7</i>	NM_017240	2986
Phospholamban	<i>PLB</i>	NM_022707	381
Ryanodine receptor II	<i>Ryr2</i>	NM_001191043	14063
Brain natriuretic peptide	<i>BNP</i>	NM_031545	234
Collagen, type I	<i>Col1a1</i>	NM_053304	4246
Collagen, type III	<i>Col3a1</i>	NM_032085	4131
Lysyl oxidase	<i>Lox</i>	NM_017061	1062
Transforming growth factor $\beta$ 1	<i>Tgfb1</i>	NM_021578	1267
Transforming growth factor $\beta$ 2	<i>Tgfb2</i>	NM_031131	1458
Transforming growth factor $\beta$ 3	<i>Tgfb3</i>	NM_031131	1397
Hypoxia inducible factor-1 $\alpha$	<i>Hif1a</i>	NM_024359	1755
Zinc finger protein GLI2	<i>Gli2</i>	NM_001107169	2352
Smoothed homolog	<i>Smo</i>	NM_012807	1971
Interleukin 6	<i>Il6</i>	NM_012589	445
Mu-crystallin	<i>Crym</i>	NM_053955	607
Aldehyde dehydrogenase, type I a I	<i>Aldh1a1</i>	NM_022407	1175
Aldehyde dehydrogenase, type I a II	<i>Aldh1a2</i>	NM_053896	1361
Aldehyde dehydrogenase, type I a III	<i>Aldh1a3</i>	NM_153300	1119
Aldehyde dehydrogenase, type II	<i>Aldh2</i>	NM_032416	1391
Glutathione-S-transferase, alpha IV	<i>Gsta4</i>	NM_001106840	816
Glutathione-S-transferase, mu I	<i>Gstm1</i>	NM_017014	364
Glutathione-S-transferase, mu II	<i>Gstm2</i>	NM_177426	340
Glutathione-S-transferase, mu IV	<i>Gstm4</i>	NM_001024304	1224
Uncoupling protein III	<i>Ucp3</i>	NM_013167	1004
Macrophage inhibitory factor	<i>Mif</i>	NM_031051	462
Angiotensin II	<i>Angpt2</i>	NM_134454	1379
Pyruvate kinase, M2	<i>Pkm2</i>	NM_053297	1438
Monocarboxylate transporter 8	<i>Slc16a2</i>	NM_147216	1561
Monocarboxylate transporter 10	<i>Slc16a10</i>	NM_138831	1528
Fatty acid translocase	<i>Cd36</i>	XM_575338	1927
Solute carrier organic anion, 1a1	<i>Slco1a1</i>	NM_017111	2618
Solute carrier organic anion, 1a4	<i>Slco1a4</i>	NM_131906	2083
Solute carrier organic anion, 1a5	<i>Slco1a5</i>	NM_030838	2217
Solute carrier organic anion, 1b3	<i>Slco1b3</i>	NM_031650	1472
Solute carrier organic anion, 2b1	<i>Slco2b1</i>	NM_080786	1789
Solute carrier organic anion, 4a1	<i>Slco4a1</i>	NM_133608	1944
Solute carrier organic anion, 4c1	<i>Slco4c1</i>	NM_001002024	2062
Large neutral amino acid transporter I (LAT1)	<i>Slc7a5</i>	NM_017353	1326
Large neutral amino acid transporter II (LAT 2)	<i>Slc7a8</i>	NM_053442	2083
4F2 cell surface antigen heavy chain (CD98)	<i>Slc3a2</i>	NM_019283	1574
Midkine	<i>Mdk</i>	NM_030859	378
Vascular endothelial growth factor A	<i>VEGFa</i>	NM_031836	1380
Endothelial nitric oxide synthase	<i>eNOS</i>	NM_021838	3563
Basic fibroblast growth factor	<i>bFGF</i>	NM_019305	897
Beta 1 adrenergic receptor	$\beta$ 1AR	NM_012701	969
Beta 2 adrenergic receptor	$\beta$ 2AR	NM_012492	337
Cyclophilin A	<i>Ppia</i>	NM_017101	486
Ribosomal protein, large, P1	<i>Rplp1</i>	NM_001007604	92
Iodothyronine deiodinase, type I	<i>DIO1</i>	NM_021653	41
Iodothyronine deiodinase, type II	<i>DIO2</i>	NM_031720	765
Iodothyronine deiodinase, type III	<i>DIO3</i>	Sequence: 5' - 3' Forward: AGAGTGGCACCATCATGTACCA Reverse: CCAAGTGCGCAACTCAGACA	

All primers obtained were from SABiosciences (Qiagen Inc., Valencia, CA) with the exception of the custom *Dio3* sequence which was obtained from Sigma Aldrich (Sigma, St. Louis, MO). The RefSeq Accession number refers to the representative sequence used to design the enclosed primers. The reference position is a position contained within the sequence of the amplicon relative to the start of the relevant RefSeq sequence.

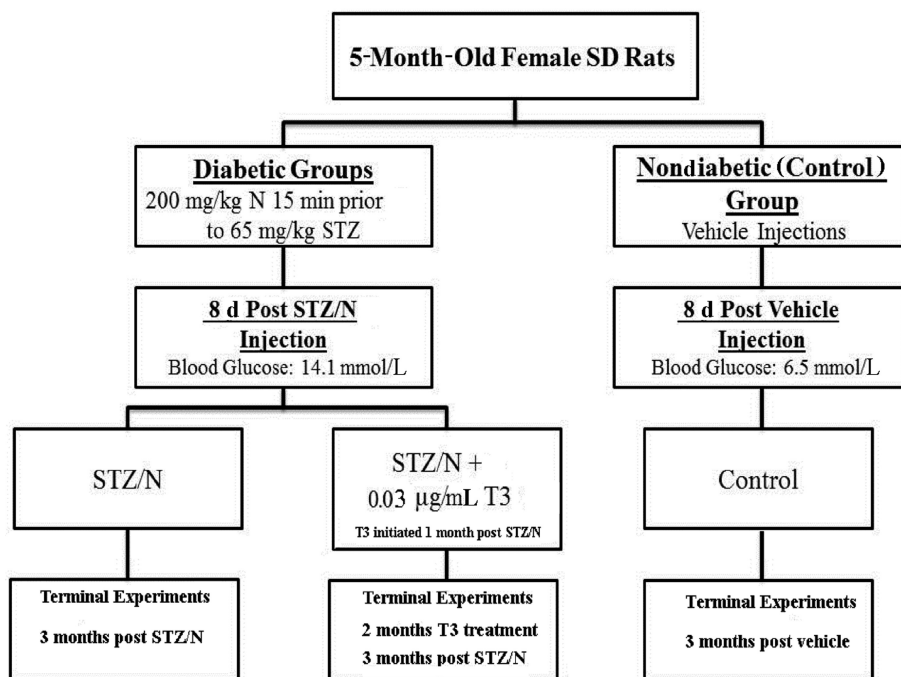
Supplementary Table S2. Physical data.

	Control	STZ/N	STZ/N-T <sub>3</sub>
n	9-10	10	9-10
BW Pre TX (g)	249 (11)	246 (24)	245 (13)
BW Post TX (g)	269 (9)	262 (33)	265 (18)
HW (mg)	1056 (65)	1048 (132)	1068 (88)
LV (mg)	735 (49)	702 (91)	720 (58)
HW/BW (mg/g)	3.93 (0.2)	4.01 (0.4)	4.04 (0.4)
LV/BW (mg/g)	2.73 (0.2)	2.69 (0.2)	2.72 (0.2)
BG (mmol/l)	13 (2)	26 (9) <sup>A</sup>	24 (9) <sup>B</sup>
Body Temp (°C)	38.1 (0.6)	38.3 (0.3)	38.3 (0.3)
HR (bpm)	353 (57)	295 (36)	333 (30)
SBP (mmHg)	145 (18)	129 (13)	144 (14)
DBP (mmHg)	85 (16)	81 (10)	84 (14)
MAP (mmHg)	115 (17)	105 (10)	113 (14)

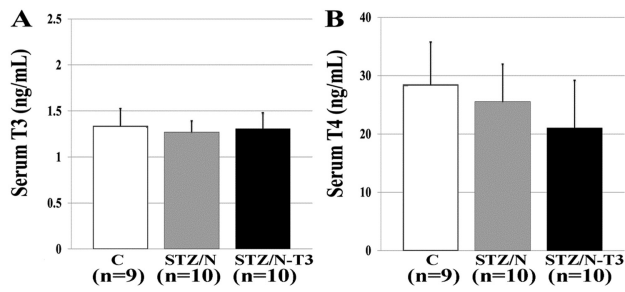
Values are means (SD); n, #/group; BW Pre TX, body weight at study initiation; BW Post TX, Body weight at terminal experiment; HW, heart weight; LV, left ventricular weight; HW/BW, heart weight/body weight ratio; LV/BW, left ventricular weight/body weight ratio; BG, blood glucose obtained from the LV; Body Temp, body temperature; HR, heart rate; SBP, systolic blood pressure; DBP, diastolic blood pressure; MAP, mean arterial pressure; <sup>A</sup>, p<0.05 vs. control; <sup>B</sup>, p<0.05 vs. STZ/N; Blood glucose samples were obtained in non-fasted animals following terminal experiments and thoracotomy.



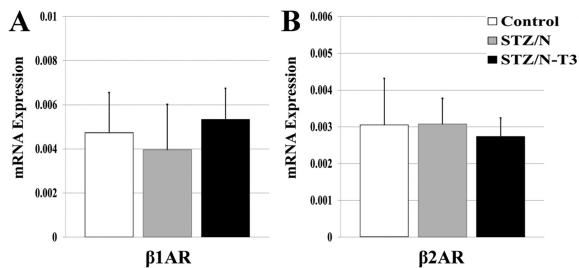
Supplementary Figure S2. Confirmation of DIO3 staining specificity. Low magnification images of serial LV sections stained with anti-DIO3 antibody (A) or Rabbit IgG negative control (B). Scale bar= 50µm; Higher magnification image of boxed area in A (C) and B (D). Scale Bar =20µm.



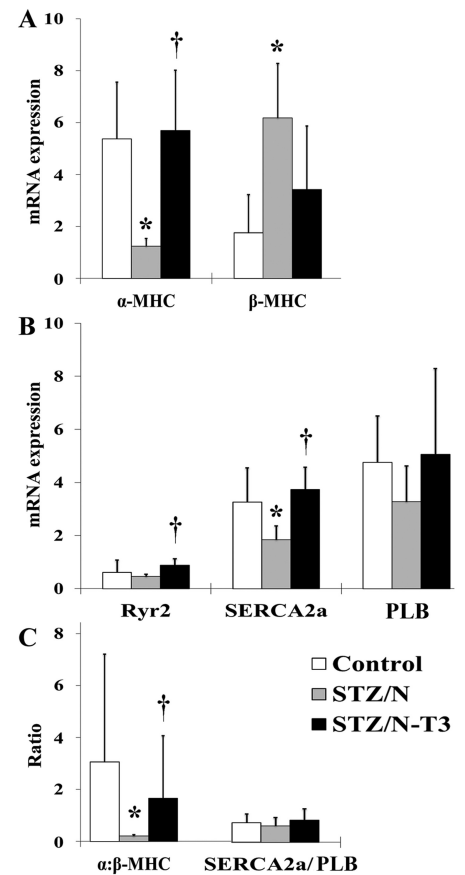
Supplementary Figure S1. Study design. Age matched female SD rats were randomly assigned to diabetic (STZ/N) or control groups. Non-insulin dependent DM was induced by STZ (65 mg/kg) following N (200 mg/kg) pre-treatment. Control animals received two vehicle injections. Eight days after induction of DM, serum blood glucose levels were tested. Diabetic rats were then randomized to diabetic control (STZ/N) or T<sub>3</sub> treatment. One month after injections to induce DM, T<sub>3</sub> treatment was initiated. Terminal data, including cardiac function, were collected from all groups two months later (3 months DM).



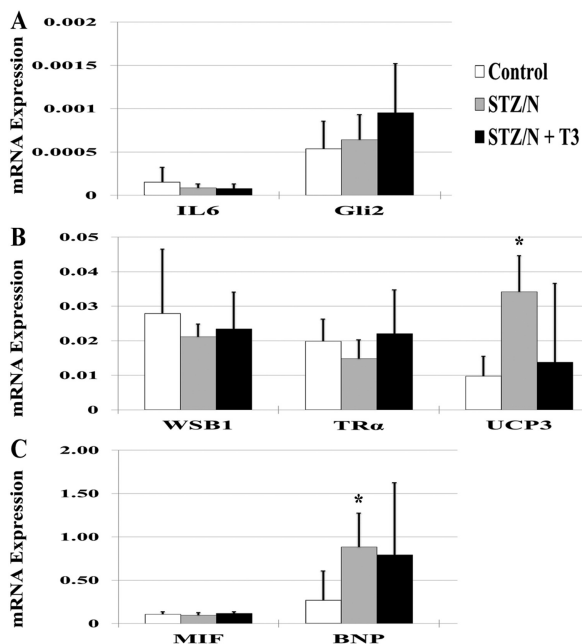
**Supplementary Figure S3.** Terminal serum total TH levels. Values represent means (SD). Serum T3, Total Triiodothyronine in serum (A); Serum T4, Total thyroxine in serum (B).



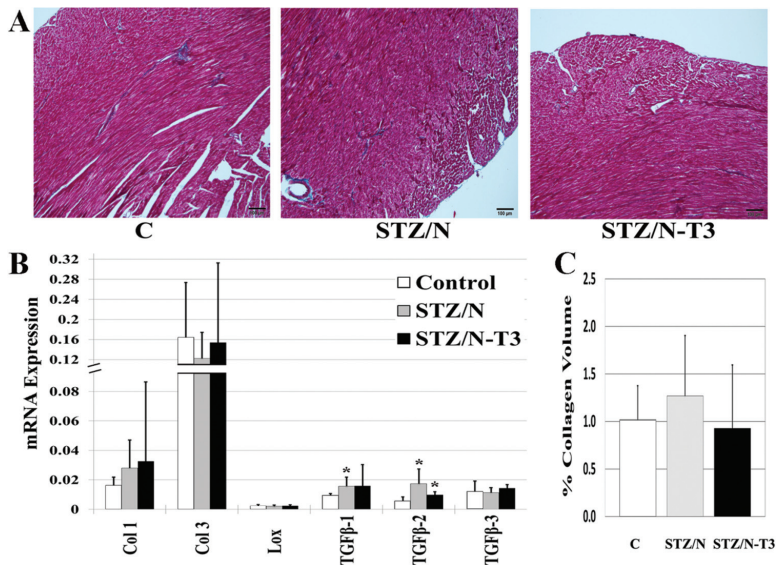
**Supplementary Figure S4.** Expression of myocardial beta adrenergic receptors. Gene expression values represented as mean (SD). Gene expression was normalized using the housekeeping genes *Cyclophilin A* and *Rplp1*.  $\beta 1AR$ , beta 1 adrenergic receptor (A);  $\beta 2AR$ , beta 2 adrenergic receptor (B); n=3-4/group.



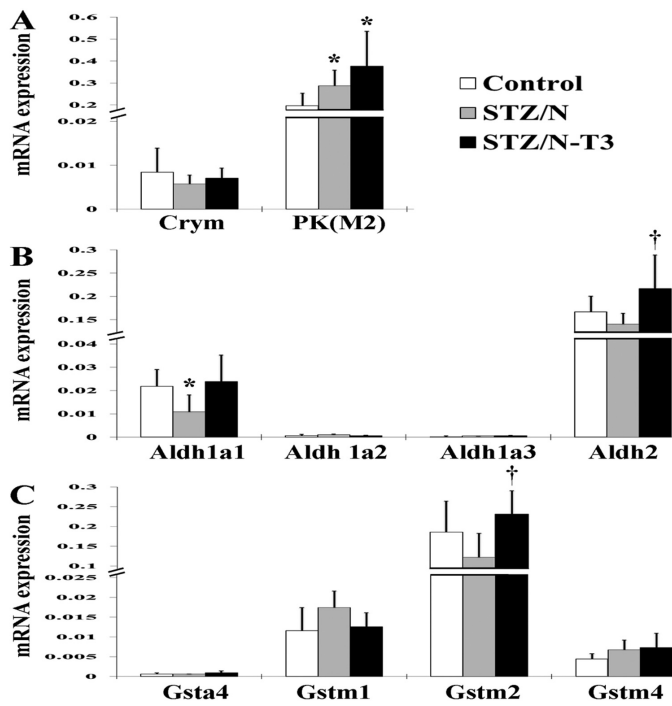
**Supplementary Figure S5.** Expression of myocardial contractility genes. Gene expression values are means (SD) or ratios of means. Gene expression was normalized using the housekeeping genes *Cyclophilin A* and *Rplp1*.  $\alpha$ -MHC,  $\alpha$ -Myosin Heavy Chain isoform (A);  $\beta$ -MHC,  $\beta$ -Myosin Heavy Chain isoform (A); *Ryr2*, Ryanodine receptor (B); *SERCA2a*, Sarco(endo)plasmic reticulum  $Ca^{2+}$ -ATPase 2a (B); *PLB*, Phospholamban (B);  $\alpha$ : $\beta$ -MHC, Ratio of  $\alpha$ -MHC to  $\beta$ -MHC expression (C); *SERCA2a/PLB*, Ratio of *SERCA2a* to *PLB* expression; n=5/group; \*, p<0.05 vs. control; †, p<0.05 vs. STZ/N.



**Supplementary Figure S6.** Normalized expression of other key myocardial genes. Gene expression values represented as mean (SD). Gene expression was normalized using the house-keeping genes *Cyclophilin A* and *Rplp1*. *IL6*, Interleukin 6 (A); *Gli2*, GLI family zinc finger 2 (A); *WSB1*, WD repeat and SOCs box-containing protein 1(B); *TR $\alpha$* , Thyroid Receptor  $\alpha$  (B); *UCP3*, Uncoupling protein 3 (B); *MIF*, Macrophage migration inhibitory factor (C); *BNP*, Brain natriuretic peptide (C); n=5/group; \*, p<0.05 vs. control; †, p<0.05 vs. STZ/N.



**Supplementary Figure S7.** LV fibrosis. Representative LV fibrosis staining by Masson's Trichrome (A; Scale Bar = 100  $\mu$ m); mRNA expression of collagens and genes known to stimulate DIO3 and/or collagen expression (B). Gene expression values represented as mean (SD); LV fibrosis quantification (C). Values represented as the proportion of collagen normalized to the total myocyte area; *Col*, Collagen; *Lox*, Lysyl Oxidase; *TGF $\beta$* , Transforming Growth Factor  $\beta$ ; n= 5-10/group; \*, p<0.05 vs. control.



**Supplementary Figure S8.** Gene expression of cytosolic TH binding proteins in the myocardium. Gene expression values represented as mean (SD). Gene expression was normalized using the housekeeping genes *Cyclophilin A* and *Rplp1*. *Crym*,  $\mu$ -crystallin (A); *PK*, Pyruvate Kinase (A); *Aldh*, Aldehyde Dehydrogenase isoforms (B); *Gst*, Glutathione S-Transferase isoforms (C); n=5/group; \*, p<0.05 vs. control; †, p<0.05 vs. STZ/N.